ResearchGate

See discussions, stats, and author profiles for this publication at: https://www.researchgate.net/publication/223410661

Theoretical and experimental study on residue curve maps of propyl acetate synthesis reaction

Article *in* Chemical Engineering Science · June 2005

DOI: 10.1016/j.ces.2005.01.023

CITATIONS
23

READS
65

4 authors, including:

Kai Sundmacher
Max Planck Institute for Dynamics of Complex Technical Systems
738 PUBLICATIONS **8,429** CITATIONS
SEE PROFILE

Dr.-Ing Samuel Kofi Tulashie
University of Cape Coast
40 PUBLICATIONS **258** CITATIONS
SEE PROFILE

Some of the authors of this publication are also working on these related projects:

InPROMPT View project

InPROMPT View project

All content following this page was uploaded by Dr.-Ing Samuel Kofi Tulashie on 23 July 2018.

The user has requested enhancement of the downloaded file.

ELSEVIER

Chemical Engineering Science 60 (2005) 3363–3371

Chemical Engineering Science

www.elsevier.com/locate/ces

Theoretical and experimental study on residue curve maps of propyl acetate synthesis reaction

Yuan-Sheng Huang[a], Kai Sundmacher[a, b, *], Samuel Tulashie[b], Ernst-Ulrich Schlünder[a]

[a] *Max-Planck-Institute for Dynamics of Complex Technical Systems, Sandtorstrasse 1, D-39106 Magdeburg, Germany*
[b] *Otto-von-Guericke-University Magdeburg, Process Systems Engineering, Universitätsplatz 2, D-39106 Magdeburg, Germany*

Received 21 July 2004; received in revised form 6 January 2005; accepted 27 January 2005
Available online 19 March 2005

Abstract

Residue curve maps (RCMs) of propyl acetate synthesis reaction in the batch reactive distillation process are studied. In order to adapt the model equations of residue curve maps to a practicable heating policy, the theoretical analysis and experimental measurements in this paper are carried out isothermally instead of the autonomous heat policy first introduced by Venimadhavan et al. (A.I.Ch.E. Journal 40 (1994) 1814–1824). The chemical equilibrium constant of this reaction is determined by experiments to be 20 within the temperature range 80–110 °C. Using this equilibrium constant, the RCMs predicted by simulation are in good agreement with the experimental measurements. The results show that there is an unstable node branch emerging from the propyl acetate–water edge, moving toward the chemical equilibrium surface with the increasing Damköhler number (*Da*), and eventually reaching the quaternary reactive azeotrope when $Da \to \infty$. Residue curves are measured with initial compositions around the unstable node, and thus the results verify the existence of this reactive azeotrope. Further bifurcation analysis shows that different heat policies will influence the singular points and topology of kinetically controlled RCMs, but not the cases when $Da = 0$ or $Da \to \infty$.
© 2005 Elsevier Ltd. All rights reserved.

Keywords: Reactive distillation; Azeotrope; Residue curve map; Bifurcation analysis; Esterification; Propyl acetate

1. Introduction

It is generally agreed that the integration of reaction and separation into a single unit (generally termed as "reactive separation process") may bring potential advantages such as reducing energy and capital cost, enhancing yield and selectivity, breaking thermodynamic restrictions and in situ purification, etc. Even though, most of these reactive separation processes are short of feasibility analysis methodologies due to process complexity. An exceptional success among these reactive separation processes is reactive distillation (RD), which has been amply studied (e.g. Taylor and Krishna, 2000; Sundmacher and Kienle, 2003). For the conceptual design of the RD process, residue curve maps (RCMs) were introduced as a very useful tool and were used by many researchers (e.g. Venimadhavan et al., 1994; Ung and Doherty, 1995; Thiel et al., 1997; Qi et al., 2002). RCMs represent the dynamic behavior of the liquid phase composition in a batch RD process. The analysis of the location and stability of the singular points in RCMs yield valuable information on the attainable products of an RD process. The existence of these stationary points was also proven experimentally (Song et al., 1997, 1998).

However, except for RD, systematic analysis for other hybrid processes combining reaction and separation has rarely been developed due to the even more complicated mix-up of reaction and mass transfer kinetics. Therefore, in our previous work (Huang et al., 2004), we proposed a methodology generalized from the distillation process to assess the effects of mass transfer kinetics on the feasible products of reactive

* Corresponding author. Tel.: +49 391 6110351; fax: +49 391 6110353.
E-mail address: sundmacher@mpi-magdeburg.mpg.de (K. Sundmacher).

0009-2509/$ - see front matter © 2005 Elsevier Ltd. All rights reserved.
doi:10.1016/j.ces.2005.01.023

membrane separation. It has been shown that the selective mass transfer effects can influence the topology of RCMs as well as the *loci* of singular points in membrane separation processes, which are termed as reactive arheotropes. When a membrane is incorporated, the isobaric operation and the autonomous heat policy (Venimadhavan et al., 1994), which was often assumed for RD, become unrealistic. Thus, to adapt the proposed generalization to reactive membrane separation, it is essential to remove the previous autonomous heat policy.

As the preliminary work for reactive membrane separation, we investigate the RCMs of RD in the present paper. The equations are reformulated to remove the constraint of autonomous heat policy, and the isothermal operation will be adopted in this work. Propyl acetate synthesis reaction is selected as the target reaction; the chemical equilibrium constant of this reaction system is determined experimentally in order to give a better prediction of the subsequent RCMs. The RCMs are first predicted by simulation and then validated by the experiments.

2. Theory

2.1. Reaction scheme and model equations of RCMs

The esterification reaction of acetic acid with propanol reads as

$$\text{Acetic acid (1)} + \text{Propanol (2)} \overset{\text{H}^+}{\longleftrightarrow} \text{Propyl acetate (3)} + \text{Water (4)}. \quad (1)$$

The rate expression can be generally expressed as

$$r = k_f(T)\Re(a), \quad (2)$$

where k_f is the temperature-dependent forward rate constant and $\Re$ denotes the dimensionless reaction rate depending on the liquid phase composition, expressed in terms of activities $a_i = x_i\gamma_i$; for heterogeneous catalyst, the adsorption term may appear in the denominator of $\Re$. In the theoretical study of kinetically controlled RCMs, quasi-homogeneous rate equations will be assumed.

Considering the batch reactive separation process depicted as Fig. 1a, the component and total mass balances are formulated in molar units as

$$\frac{\mathrm{d}(Hx_i)}{\mathrm{d}t} = -n_i + v_i H_r k_f \Re, \quad i = 1 \ldots \mathrm{NC}-1, \quad (3)$$

$$\frac{\mathrm{d}H}{\mathrm{d}t} = -n_T + v_T H_r k_f \Re, \quad (4)$$

where H represents the total molar liquid holdup, H_r the holdup in which the reaction proceeds, n_i the component molar flow rate, $n_T = \sum_{i=1}^{\mathrm{NC}} n_i$ the total molar flow rate, v_i the stoichiometric coefficient of component i, and $v_T = \sum_{i=1}^{\mathrm{NC}} v_i$ the total mole change of the chemical reaction.

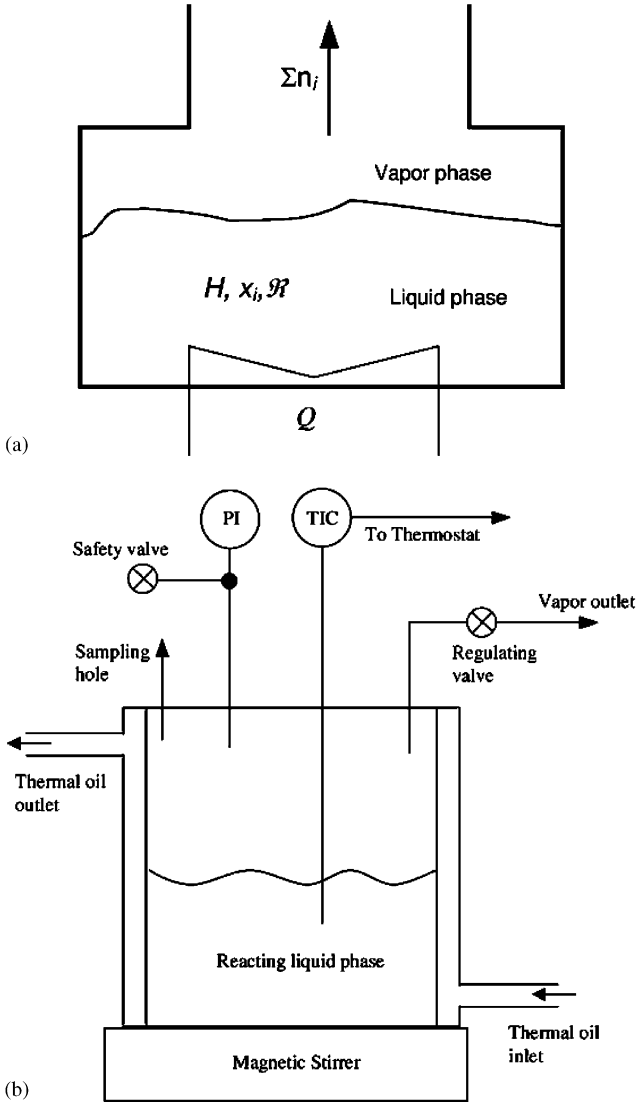

Fig. 1. (a) A generalized sketch for reactive separation. (b) Experimental setup.

Rearranging the above equations and introducing the dimensionless Damköhler number yield (Huang et al., 2004)

$$\frac{\mathrm{d}x_i}{\mathrm{d}\xi} = \left(x_i - \frac{n_i}{n_T}\right) + Da(v_i - v_T x_i)\,\frac{H_r}{H_{r,0}}\,\frac{n_{T,\mathrm{ref}}}{n_T}\,\frac{k_f}{k_{f,\mathrm{ref}}}\,\Re, \quad (5)$$

where ξ stands for the dimensionless time with $\mathrm{d}\xi = (n_T/H)\,\mathrm{d}t$, $H_{r,0}$ is the initial reactive holdup, and $n_{T,\mathrm{ref}}$ and $k_{f,\mathrm{ref}}$ are the total molar flow rate and the forward reaction rate constant at a reference point within the composition space, in this work chosen as the propanol apex. *Da*, the Damköhler number, is defined as the ratio of the characteristic reaction rate ($H_{r,0}k_{f,\mathrm{ref}}$) and the characteristic escaping total flux $n_{T,\mathrm{ref}}$:

$$Da \equiv \frac{H_{r,0}k_{f,\mathrm{ref}}}{n_{T,\mathrm{ref}}}. \quad (6)$$

With different operating conditions, Eq. (5) can be further reduced:

$$\frac{dx_i}{d\xi} = \left(x_i - \frac{n_i}{n_T}\right) + Da(v_i - v_T x_i)\,\frac{k_f}{k_{f,\mathrm{ref}}}\,\Re$$

(autonomous heat strategy), (7a)

$$\frac{dx_i}{d\xi} = \left(x_i - \frac{n_i}{n_T}\right) + Da(v_i - v_T x_i)\,\frac{n_{T,\mathrm{ref}}}{n_T}\,\frac{k_f}{k_{f,\mathrm{ref}}}\,\Re$$

(non-volatile catalyst), (7b)

$$\frac{dx_i}{d\xi} = \left(x_i - \frac{n_i}{n_T}\right) + Da(v_i - v_T x_i)\,\frac{H_r}{H_{r,0}}\,\frac{n_{T,\mathrm{ref}}}{n_T}\,\Re$$

(isothermal condition). (7c)

For the considered isothermal and heterogeneously catalytic reaction in this work, it becomes

$$\frac{dx_i}{d\xi} = \left(x_i - \frac{n_i}{n_T}\right) + Da(v_i - v_T x_i)\,\frac{n_{T,\mathrm{ref}}}{n_T}\,\Re. \quad (7d)$$

The advantage of using the flux notation n_i, n_T is that the mass transfer kinetics of the separation process can be considered subordinately. Therefore, the formulation up to Eq. (7d) is applicable to non-equilibrium separation processes, e.g. when there exists an inert gas film in the vapor phase (Schlünder, 1979) or when a selective membrane is incorporated (Huang et al., 2004). Only in a very specific case of open distillation, the flux ratio (n_i/n_T) equals the vapor mole fraction y_i, which is assumed to be in phase equilibrium with x_i, and the total molar flow rate is usually denoted as V, which is proportional to the total vapor pressure of the system.

$$\frac{dx_i}{d\xi} = (x_i - y_i) + Da(v_i - v_T x_i)\,\frac{V_{\mathrm{ref}}}{V}\,\Re. \quad (8)$$

Eq. (8) will be used to study the RCMs of distillation process at non-reactive, kinetically controlled, and equilibrium reactive conditions.

2.2. Vapor–liquid equilibria

Taking account of the dimerization reaction of acetic acid in the vapor phase, the mole fraction y_i can be calculated by

$$y_i P z_i = x_i \gamma_i(x_j, T)\, p_i^{\mathrm{sat}}(T), \quad (9)$$

where the saturated pressures (p_i^{sat}) are calculated by the Antoine equation, and the liquid phase activity coefficients (γ_i) are calculated by the NRTL equation (Gmehling and Onken, 1977). z_i are the dimerization correction factors described by Marek and Standart (1954) and Barbosa and Doherty (1988a). For detailed information of the thermodynamic model, refer to the Appendix.

2.3. Equilibrium constant

Due to the fact that the equilibrium constant calculated by the extrapolation of literature data (Krishnaiah and Bhagvanth Rao, 1984; Bart et al., 1996) does not result in a good prediction of RCMs, K_{eq} has been determined experimentally, using the following equation:

$$K_{\mathrm{eq}} = \frac{a_{\mathrm{PrAc}} a_{\mathrm{H_2O}}}{a_{\mathrm{AcAc}} a_{\mathrm{PrOH}}} = \frac{x_{\mathrm{PrAc}} x_{\mathrm{H_2O}}}{x_{\mathrm{AcAc}} x_{\mathrm{PrOH}}}\,\frac{\gamma_{\mathrm{PrAc}} \gamma_{\mathrm{H_2O}}}{\gamma_{\mathrm{AcAc}} \gamma_{\mathrm{PrOH}}} = K_{\mathrm{eq},x} K_{\mathrm{eq},\gamma}. \quad (10)$$

3. Experiment

3.1. Chemicals

Acetic acid (99–100%, Merck), propanol (> 99%, Merck) and propyl acetate (> 98%, Merck) were used as reactants; the commercial ion exchange resin (Amberlyst® 15, Merck) was used to catalyze the reaction.

3.2. Apparatus

The experiments were carried out in a steel-jacketed vessel (stainless steel 316Ti, material number 1.4571) of 1.57 L volume (10 cm inner diameter × 20 cm height) as shown in Fig. 1b. It is operated in batch mode, magnetically stirred at 300 rpm, and equipped with temperature and pressure sensors, a regulating valve and a blow-off safety valve. The temperature was controlled by a thermostat (Julabo, F30-C). Samples were taken via the sampling hole, which was sealed with a silicone pad; the syringe capped with the 30-cm-long needle (Rettberg, Germany) pierced through the pad to take samples from the reacting liquid phase.

3.3. Analysis of composition

The samples were analyzed by gas chromatography (Hewlett-Packard, HP6890 series) and the mixtures were separated in a cross-linked polyethylene glycol column (HP-INNOWAX, Part No. 19091N-133). The column temperature was programmed with a 2 min initial hold at 50 °C, followed by a 50 °C/min ramp up to 130 °C and held for 2.5 min. Both the thermal conductivity detector (TCD) and the flame ionization detector (FID) were used for peak detection. Due to the fact that propanol and water have an inseparable peak time, the water amount was calculated by the subtraction of TCD and FID signals. To guarantee a controlled error of such a subtraction method, the GC was recalibrated when the compositions calculated by TCD and FID differed from each other above 1.5%.

3.4. Determination of equilibrium constant

The chemical equilibrium constant was measured within a temperature range of 80–110 °C. Acetic acid and propanol of different initial ratios were prepared, with a total volume of 150 mL. The mixture was poured into the reactor and 5 g Amberlyst 15 was added to catalyze the reaction. The reactor was then closed and heated to the set temperature. Samples

were taken every certain time interval, and equilibrium was judged to be reached when the concentration profile was eventually flat.

3.5. Residue curves measurement

According to the simulation result shown later in Section 4.2, there exists an unstable node, a quaternary reactive azeotrope, at the reactive condition. Residue curves were measured to validate this prediction.

Mixtures of initial compositions close to the unstable node were prepared to start a residue curve. The mixture and catalyst were added into the reactor, closed and heated up to the set temperature, 105 °C. The liquid compositions were measured by taking samples (∼ 0.5 mL/sample) every 10 min, analyzed by gas chromatography. When the liquid residue amount was too small to take any more samples, this run was ended. The subsequent run started with the initial composition close to the final point of the previous run. Several runs were repeated until they constituted a sufficient portion of one residue curve. To guarantee the sufficiently high *Da*, the relationship of catalyst concentration and escaping flow rate was checked. The escaping flow rate was controlled ∼ 40 mL/h by the regulating valve; under this condition, 25 g dry catalyst in 300 mL initial liquid volume could approach the prediction well. To give the safety factor of 20%, 30 g catalyst was used in the initial liquid volume of 300 mL in this work.

Due to the partial solubility between propyl acetate and water, the liquid phase splitting issue was carefully checked when taking every sample (Okasinski and Doherty, 2000), even though the phase splitting was not observed through the whole experiments.

4. Results

4.1. The chemical equilibrium constant

The experimental data of chemical equilibrium composition are listed in Table 1, and the equilibrium constant was calculated by Eq. (10). According to the results, the temperature dependency of equilibrium constant was very weak and could not de facto be determined within the temperature range of experiments. The average value of 20 was used in the theoretical prediction of RCMs, which showed a fairly good agreement with the experimental measurement.

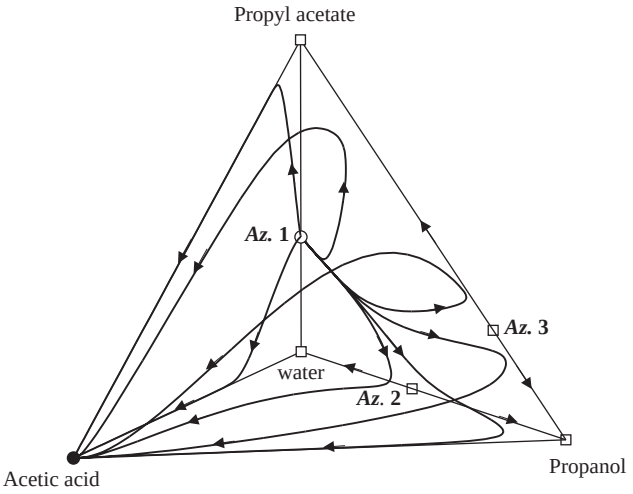

Fig. 2. RCM of simple distillation for the propyl acetate system at 105 °C ($Da = 0$) (◯ unstable node, □ saddle point, ● stable node).

4.2. Prediction of RCMs by simulation

Fig. 2 shows the RCM for non-reactive distillation at 105 °C. There are three non-reactive binary azeotropes in the RCM. The azeotrope between propyl acetate and water (Az. 1) is the unstable node, while the other two (Az. 2 and Az. 3) are the saddle points. Pure propanol, propyl acetate and water are also saddle points, and acetic acid is the only stable node for the simple distillation. Residue curves originate from the unstable node, first approaching the saddle points, and finally converge to the stable node. The information of all singular points is listed in Table 2.

When $Da = 1$ (as Fig. 3), Az. 2 and Az. 3 still retain their positions and stability, while the unstable node (Az. 1) no longer exists since propyl acetate and water start reacting. Instead, the unstable node moves into the composition tetrahedron and becomes the quaternary kinetic azeotrope. Moreover, the propanol apex becomes a stable node instead of a saddle point.

At $Da \rightarrow \infty$ (as Fig. 4), the reaction approaches its chemical equilibrium and the residue curves are first dominated by the reaction stoichiometry and then move along the

Table 1
Experiment results on equilibrium constant determination (initial liquid volume: 150 mL, 5 g catalyst)

T (°C)	$x_{1,0}/x_{2,0}$	$x_{1,e}$	$x_{2,e}$	$x_{3,e}$	$x_{4,e}$	$\gamma_{1,e}$	$\gamma_{2,e}$	$\gamma_{3,e}$	$\gamma_{4,e}$	$K_{eq,x}$	$K_{eq,\gamma}$	K_{eq}
80	0.5/0.5	0.1617	0.1617	0.3383	0.3383	0.7483	1.1610	1.5933	2.4459	4.377	4.488	19.643
80	0.2/0.8	0.0186	0.6186	0.1814	0.1814	0.6385	1.0448	1.6083	3.0952	2.860	7.486	21.409
80	0.8/0.2	0.6105	0.0105	0.1895	0.1895	0.9742	0.9884	1.6082	1.8727	5.602	3.119	17.474
95	0.5/0.5	0.1573	0.1573	0.3427	0.3427	0.7507	1.1645	1.5912	2.4291	4.746	4.419	20.971
110	0.5/0.5	0.1582	0.1582	0.3418	0.3418	0.7573	1.1629	1.5881	2.4078	4.668	4.342	20.267

Table 2
List of singular points in Figs. 2–4

Name	Composition	Type	Pressure (bar)	*Da*			x_1	x_2	x_3
				0	1	∞			
Azeotrope 1	$PrAc/H_2O$	Unstable	2.38	√			0	0	0.3774
Azeotrope 2	$PrOH/H_2O$	Saddle	1.91	√	√	√	0	0.4347	0
Azeotrope 3	PrOH/PrAc	Saddle	1.44	√	√	√	0	0.7311	0.2689
Azeotrope 4	$AcAc/PrOH/PrAc/H_2O$	Unstable	2.29		√		0.0210	0.1193	0.2929
Azeotrope 5	$AcAc/PrOH/PrAc/H_2O$	Unstable	2.06			√	0.0599	0.3331	0.1260
Propanol	PrOH	Saddle/Stable	1.35	√	√	√	0	1	0
Water	H_2O	Saddle	1.20	√	√	√	0	0	0
Propyl acetate	PrAc	Saddle	1.13	√	√	√	0	0	1
Acetic acid	AcAc	Stable	0.67	√	√	√	1	0	0

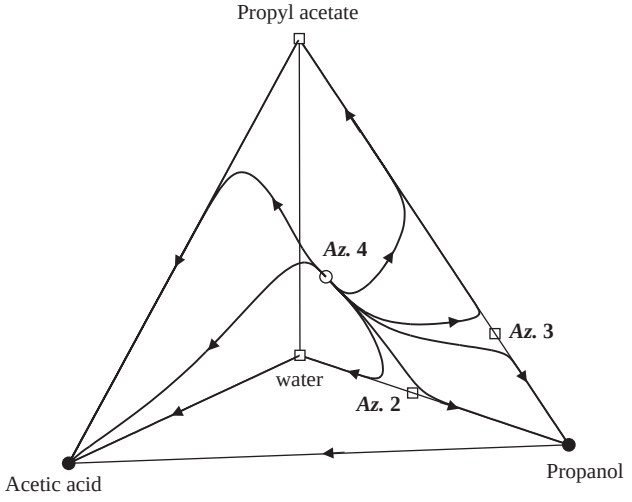

Fig. 3. RCM of kinetically controlled RD for the propyl acetate system at 105 °C ($Da = 1$) (◯ unstable node, □ saddle point, ● stable node).

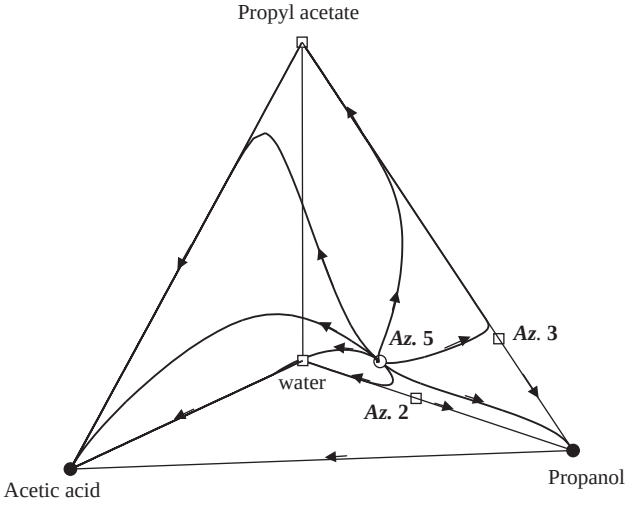

Fig. 4. RCM of equilibrium-controlled RD for the propyl acetate system at 105 °C ($Da \to \infty$) (◯ unstable node, □ saddle point, ● stable node).

equilibrium surface (as Fig. 5) to the stable node. The unstable node meets a saddle point branch, which emerges from the propanol–water edge (when $Da > 3.54$), on the

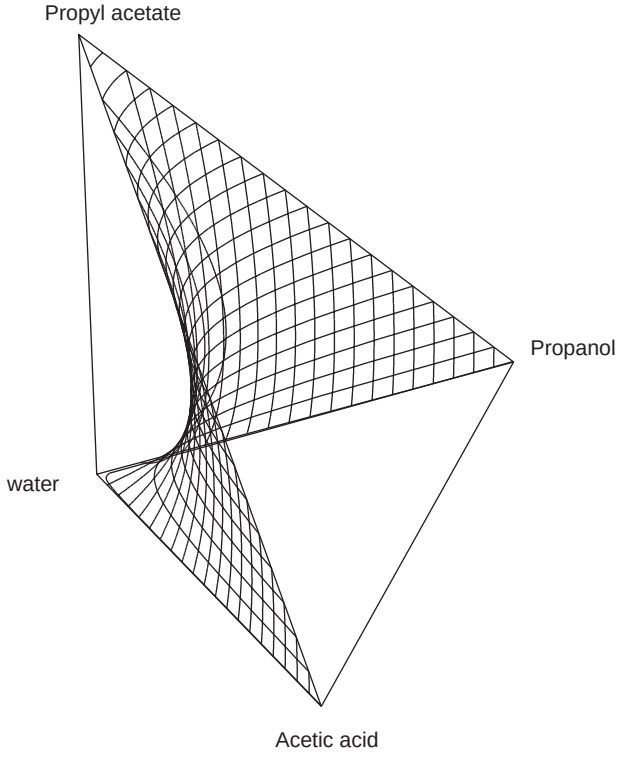

Fig. 5. Surface of chemical equilibrium composition for the propyl acetate system at 105 °C ($K_{eq} = 20$).

equilibrium surface and results in the quaternary reactive azeotrope.

4.2.1. Bifurcation analysis

Fig. 6 shows the bifurcation behavior of simple reactive distillation. The binary azeotrope between propyl acetate and water, Az. 1, moves into the composition tetrahedron when chemical reaction takes place ($Da > 0$). On the other hand, the binary azeotropes of propanol–water (Az. 2) and propanol–propyl acetate (Az. 3) still remain in reactive cases since these binary pairs do not react with each other. However, a saddle point branch emerges from Az. 2 when *Da* is larger than a critical value about 3.54, and then meets the

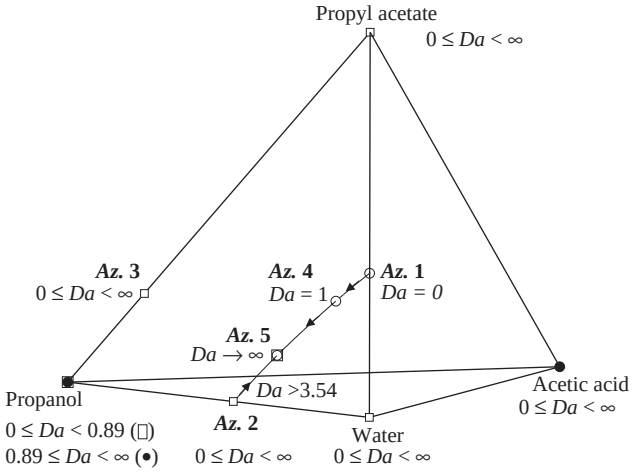

Fig. 6. Singular point *loci* and bifurcation behavior for RD at 105 °C (◯ unstable node, □ saddle point, ● stable node).

unstable node branch at the reactive azeotrope when $Da \rightarrow \infty$. The other singular points retain their positions and stability at any *Da*, except that propanol changes from a saddle point to a stable node when *Da* exceeds the critical value, 0.89.

Fig. 7a also shows the bifurcation behavior, but in the form of pressure versus the normalized Damköhler number, $Da/(Da+1)$. It shows that in the non-reactive case, Az. 1 is the lightest component and therefore the unstable node, while acetic acid has the lowest pressure and behaves as the stable node. With increasing *Da*, Az. 1 does not remain but moves toward the reactive azeotrope (Az. 5) instead. When $Da > 0.89$, propanol becomes another stable node in addition to acetic acid. When $Da > 3.54$, there appears another quaternary azeotrope as a saddle point, which will join the reactive azeotrope eventually when $Da \rightarrow \infty$.

4.2.2. Influence of isothermal and autonomous heat policies

The different operating policies of Eq. (7) would influence the relative weighting of the separation term (the first term on the right-hand side of Eq. (7)) and the reaction term (the second term on the right-hand side) and therefore could change the topology of the RCMs.

Fig. 7b shows the similar bifurcation analysis (as Fig. 7a) but for the autonomous heat policy assuming that the k_f is independent of temperature. It can be seen that at both extreme cases when $Da = 0$ or $Da \rightarrow \infty$, the singular points are not affected by the heat policies. However, for kinetically controlled cases, the location of singular points could be different at a specific *Da* (depicted as dashed and dotted lines in Fig. 7b). Nevertheless, the singular point *loci* in the composition tetrahedron (as Fig. 6) will not be influenced neither. One can imagine that the swing of escaping flow rate (V_{ref}/V in Eq. (8)) together with the *Da* number result in the effective factor representing the ratio of the reaction rate and the mass transfer rate.

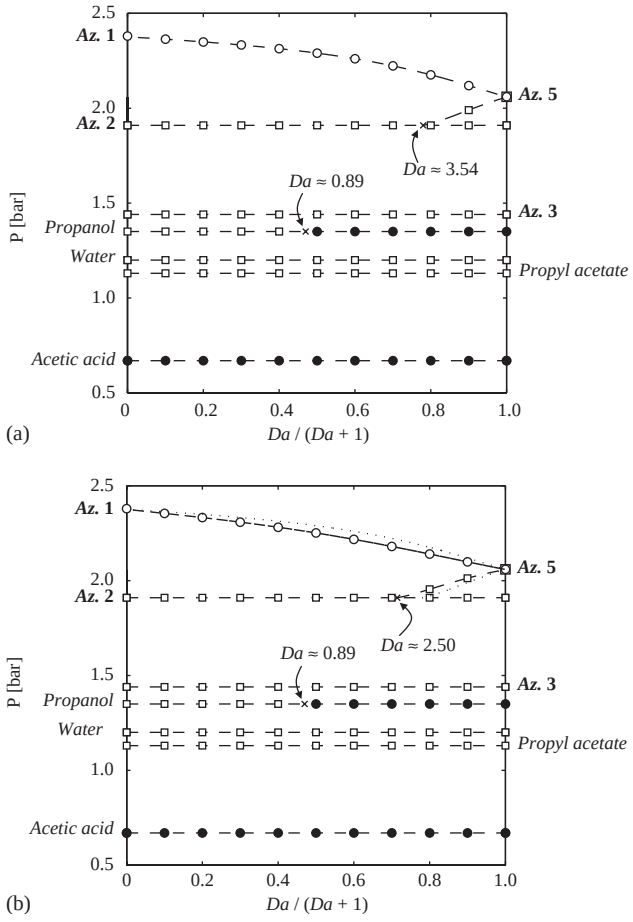

Fig. 7. (a) Bifurcation behavior of RD at 105 °C, in the form of pressure versus normalized *Da*. (b) Bifurcation diagram comparing the autonomous (dashed line) and isothermal (dotted line) heating policies (◯ unstable node, □ saddle point, ● stable node).

4.3. Experimental validation of reactive azeotrope

Experiments were carried out to validate the reactive azeotrope (Az. 5) and the results are plotted as in Fig. 8. For better visualization, the transformed variable coordinate is used (Barbosa and Doherty, 1988b), where propyl acetate is selected as the reference component:

$$X_A = x_{\text{AcAc}} + x_{\text{PrAc}},$$

$$X_B = x_{\text{PrOH}} + x_{\text{PrAc}},$$

$$X_C = x_{\text{H}_2\text{O}} - x_{\text{PrAc}} = 1 - X_A - X_B. \tag{11}$$

Different residue curves were designated by different symbols, and different colors in one curve represent different runs of experiments. A total of 36 runs were performed to constitute eight curves originating around the reactive azeotrope whose molar fraction is 5.99% acetic acid, 33.31% propanol, 12.60% propyl acetate and 48.10% water. The liquid composition changes slowly near the unstable node so that data points cluster closely. The experimental results are in good agreement with the prediction and

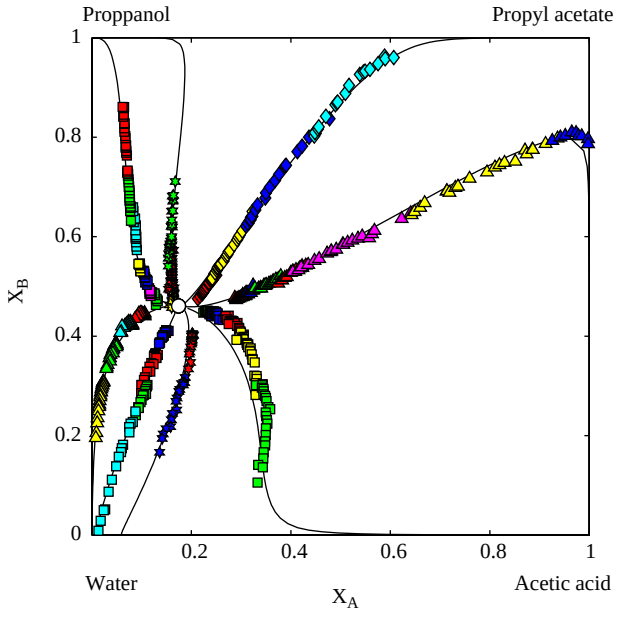

Fig. 8. Experimental validation of RCM in Fig. 4, in the form of transformed composition coordinate ($T = 105\,^{\circ}\mathrm{C}$).

again validate the existence of reactive azeotrope under the isothermal operation.

5. Conclusion

In this work, the residue curve maps of the propyl acetate system are studied, whose equilibrium constant was determined to be 20 experimentally. The simulations and experimental measurement of RCMs were carried out isothermally to remove the autonomous heat policy restriction. It has been shown that different heat policies do not affect the RCMs at non-reactive ($Da = 0$) and equilibrium-controlled reactive ($Da \to \infty$) conditions. However, it does influence the kinetically controlled RCMs ($0 < Da < \infty$) because the swing of escaping flow rate changes the ratio of reaction rate and mass transfer rate.

The results show that there are different kinds of singular points in the propyl acetate system as listed in Table 2. Most of these singular points are saddle; the only unstable node emerges from the binary azeotrope of propyl acetate and water at non-reactive condition, moves into the composition tetrahedron with increasing *Da*, and finally reaches the quaternary reactive azeotrope. Acetic acid is the only stable node of the system when $Da < 0.89$, and propanol becomes the other stable node when *Da* increases further.

Residue curves were then measured for the equilibrium-controlled reactive condition, and each curve was started with the initial composition around the quaternary reactive azeotrope. The results are in good agreement with the prediction, and thus validate the existence of reactive azeotrope under the isothermal condition.

Notation

a_i	liquid phase activity of component *i*
Da	Damköhler number, Eq. (6)
H	molar liquid holdup, mol
H_0	initial molar liquid holdup, mol
H_r	holdup in which the reaction proceeds, mol
$H_{r,0}$	initial holdup in which the reaction proceeds, mol
k_A	dimerization equilibrium constant, 1/Pa
k_f	forward reaction rate constant, 1/s
$k_{f,\mathrm{ref}}$	forward reaction rate constant at reference temperature, 1/s
K_{eq}	chemical equilibrium constant
n_i	molar flow rate of component *i* through membrane, mol/s
n_T	total molar flow rate through membrane, mol/s
$n_{T,\mathrm{ref}}$	total molar flow rate at a reference state, mol/s
NC	number of reacting species
$N_{i,j}$	interaction parameter for NRTL model, Table 3
p_i^{sat}	saturated vapor pressure of component *i*, Pa
P	system pressure, Pa
r	reaction rate, mol/(mol s)
R	universal gas constant, 8.314 J/(mol K)
$\Re$	dimensionless reaction rate, Eq. (2)
t	time, s
T	temperature, K
V	total molar flow rate for open evaporation process, mol/s
V_{ref}	total molar flow rate at a reference state, mol/s
x_i	liquid phase mole fraction of component *i*
X_A, X_B, X_C	transformed liquid phase mole fraction of component *i*, Eq. (11)
y_i	mole fraction of component *i* in vapor phase
z_i	dimerization correction factor, Eq. (9)

Greek letters

α_{ij}	interaction parameter for NRTL model, Table 3
γ_i	activity coefficient of component *i*
v_i	stoichiometric coefficient of component *i*
v_T	total mole change of reaction
ξ	dimensionless time, $\mathrm{d}\xi = (n_T/H)\,\mathrm{d}t$

Subscripts

AcAc	acetic acid
H_2O	water
i, *j*	components *i*, *j*
PrAc	propyl acetate
PrOH	propanol
1, 2, 3, 4	acetic acid, propanol, propyl acetate, water

Table 3
Thermodynamic data for the propyl acetate system

Component	Acetic acid	Propanol	Propyl acetate	Water
Normal boiling point (K)	391.15	370.35	374.65	373.15
Antoine coefficients				
A	22.1001	22.72435	21.6266	23.2256
B	−3654.62	−3310.394	−3249.98	−3835.18
C	−45.392	−74.687	−52.84	−45.343
Dimerization constants				
D_1	−12.5459	—	—	—
D_2	3166.0	—	—	—
NRTL coeff. (N_{ij})	j = acetic acid	j = propanol	j = propyl acetate	j = water
i = acetic acid	—	−147.4298	−410.3887	−342.1961
i = propanol	104.1007	—	1055.3593	152.5084
i = propyl acetate	1050.5581	−433.1348	—	720.1784
i = water	1175.7145	1866.3369	3497.7669	—
NRTL coeff. (α_{ij})	j = acetic acid	j = propanol	j = propyl acetate	j = water
i = acetic acid	—	0.3007	0.2970	0.2952
i = propanol	0.3007	—	0.3011	0.3747
i = propyl acetate	0.2970	0.3011	—	0.2942
i = water	0.2952	0.3747	0.2942	—

Abbreviations

RCM	residue curve map
RD	reactive distillation
RMS	reactive membrane separation

Appendix A

In Eq. (9), the saturated vapor pressure of each component is calculated by the Antoine equation:

$$\ln\, p_1^{\text{sat}} = A + \frac{B}{T + C} \quad (p_1^{\text{sat}} \text{ in Pa}, \quad T \text{ in K}). \tag{A.1}$$

The dimerization correction factor (z_i) is calculated using the following equations:

$$z_A = \frac{1 + (1 + 4k_A p_1^{\text{sat}})^{0.5}}{1 + (1 + 4k_A P y_A (2 - y_A))^{0.5}} \tag{A.2}$$

for the associating molecule (acetic acid), and

$$z_N = \frac{2(1 - y_A + (1 + 4k_A P y_A (2 - y_A))^{0.5})}{(2 - y_A)(1 + (1 + 4k_A P y_A (2 - y_A))^{0.5})} \tag{A.3}$$

for the other three components, where k_A, the dimerization equilibrium constant, is calculated by

$$\log_{10} k_A = D_1 + \frac{D_2}{T} \quad (k_A \text{ in Pa}^{-1}, \quad T \text{ in K}). \tag{A.4}$$

The thermodynamic data are listed in Table 3.

References

Barbosa, D., Doherty, M.F., 1988a. The influence of equilibrium chemical reactions on vapor–liquid phase diagrams. Chemical Engineering Science 43, 529–540.

Barbosa, D., Doherty, M.F., 1988b. The simple distillation of homogeneous reactive mixtures. Chemical Engineering Science 43, 541–550.

Bart, H.J., Kaltenbrunner, W., Landschützer, H., 1996. Kinetics of esterification of acetic acid with propyl alcohol by heterogeneous catalysis. International Journal of Chemical Kinetics 28, 649–656.

Gmehling, J., Onken, U., 1977. Vapour–Liquid Equilibrium Data Collection, Chemistry Data Series. Frankfurt am Main, DECHEMA.

Huang, Y.-S., Sundmacher, K., Qi, Z., Schlünder, E.-U., 2004. Residue curve maps of reactive membrane separation. Chemical Engineering Science 59, 2863–2879.

Krishnaiah, D., Bhagvanth Rao, M., 1984. Kinetics of esterification of n-propyl alcohol with acetic acid catalysed by Dowex-50w. Indian Journal of Technology 22, 268–271.

Marek, J., Standart, G., 1954. Vapor–liquid equilibria in mixtures containing an associating substance. I. Equilibrium relationships for systems with an associating component. Collection of Czechoslovak Chemical Communications, English Edition 19, 1074–1084.

Okasinski, M.J., Doherty, M.F., 2000. Prediction of heterogeneous reactive azeotropes in esterification systems. Chemical Engineering Science 55, 5263–5271.

Qi, Z., Kolah, A., Sundmacher, K., 2002. Residue curve maps for reactive distillation systems with liquid phase splitting. Chemical Engineering Science 57, 163.

Schlünder, E.-U., 1979. The effect of diffusion on the selectivity of entraining distillation. International Chemical Engineering 19, 373–379.

Song, W., Huss, R.S., Doherty, M.F., Malone, M.F., 1997. Discovery of a reactive azeotrope. Nature 388, 561.

Song, W., Venimadhavan, G., Manning, J.M., Malone, M.F., Doherty, M.F., 1998. Measurement of residue curve maps and heterogeneous kinetics in methyl acetate synthesis. Industrial & Engineering Chemistry Research 37, 1917.

Sundmacher, K., Kienle, A., 2003. Reactive Distillation—Current Status and Future Directions. Wiley–VCH, Weinheim, Germany.

Taylor, R., Krishna, R., 2000. Modelling reactive distillation. Chemical Engineering Science 55, 5183–5229.

Thiel, C., Sundmacher, K., Hoffmann, U., 1997. Residue curve maps for hetero-geneously catalysed reactive distillation of fuel ethers MTBE and TAME. Chemical Engineering Science 52, 993–1005.

Ung, S., Doherty, M.F., 1995. Calculation of residue curve maps for mixtures with multiple equilibrium chemical reactions. Industrial & Engineering Chemistry Research 34, 3195.

Venimadhavan, G., Buzad, G., Doherty, M.F., Malone, M.F., 1994. Effect of kinetics on residue curve maps for reactive distillation. A.I.Ch.E. Journal 40, 1814–1824.

View publication stats